Mater. Res. Soc. Symp. Proc. Vol. 1712 © 2014 Materials Research Society
DOI: 10.1557/opl.2014.540

Advances in Crystallographic Image Processing for Scanning Probe Microscopy: Unambiguous identification of the translation symmetry of a 2D periodic image

Taylor T. Bilyeu, Jack C. Straton, Axel Mainzer Koenig, and Peter Moeck*
Nano-Crystallography Group, Department of Physics, Portland State University, Portland, OR 97207-0751, U.S.A, *corresponding author's email: pmoeck@pdx.edu

ABSTRACT

A statistically sound procedure for the unambiguous identification of the underlying Bravais lattice of an image of a 2D periodic array of objects is described. Our Bravais lattice detection procedure is independent of which type of microscope has been utilized for the recording of the image data. It is particularly useful for the correction of Scanning Tunneling Microscope (STM) images that suffer from a blunt scanning probe tip artifact, i.e. simultaneously recording multiple mini-tips. The unambiguous detection of the type of translation symmetry presents a first step towards making objective decisions about which plane symmetry a 2D periodic image is best modeled by. Such decisions are important for the application of Crystallographic Image Processing (CIP) techniques to images from Scanning Probe Microscopes (SPMs).

INTRODUCTION

CIP is well established in the electron microscopy community, having been utilized for the analysis and enhancement of high-resolution transmission electron microscope images of crystals and quasi-2D periodic arrays of membrane proteins. The technique has recently been adapted to the processing of 2D periodic images from SPMs [1-9]. A novel procedure for the unambiguous identification of the underlying Bravais lattice of an experimental or simulated image of a 2D periodic array of objects (e.g. molecules or atoms and their respective electron density distribution functions) is part of these adaptations [7]. This procedure is described briefly in this paper and constitutes a partial solution to an unresolved issue in CIP. That unresolved issue is the complete quantification of the deviations of 2D periodic images from the space group symmetries that are allowed in the Euclidian plane so that unambiguous decisions can be made about which plane symmetry a 2D periodic image is best modeled by. The outlook section of this paper will briefly outline a way to fully resolve this issue in future work.

METHODS

Crystallographic image processing and traditional plane symmetry deviation quantifiers

In order to determine the plane symmetry to which a 2D periodic image most likely belongs, one traditionally utilizes Fourier coefficient (FC) amplitude (A_{res}) and phase angle (φ_{res}) residuals [3,10]. These values quantify how much an unprocessed image deviates from a symmetrized (fully CIP processed) one, and thus serve as figures of merit for determining which plane symmetry group best models the image (and the sample being imaged).

There is, however, no fully objective way to use these two residuals to assign the correct plane symmetry group to an image. This is because higher symmetric plane groups (such as *p4mm*) possess a higher multiplicity of the general position per primitive unit cell than their type I subgroups (such as *p4*, *c2mm* and *p2mm*). These subgroups are formed from their type I supergroup by the removal of certain symmetry operations [11]. Whenever the FC residuals of an image are not significantly larger for a particular plane group than for its respective type I subgroups, one would generally conclude that this particular group is the more likely plane group, in comparison to other groups in its subgroup/supergroup tree.

In addition to the FC amplitude and phase angle residuals, it is also customary to utilize the so called A_o/A_e ratio [3,9] for those six plane symmetry groups that possess systematic absences. This ratio is defined as the amplitude sum of the Fourier coefficients that are forbidden by the plane symmetry but were nevertheless observed (A_o), divided by the amplitude sum of all other observed Fourier coefficients that are allowed by the plane symmetry, (A_e). For the six plane symmetry groups to which this ratio is applicable, a larger value makes it more unlikely that the corresponding group is the right plane symmetry group when geometric distortions and other sources of correctable systematic errors are removed. However, the application of this plane symmetry deviation quantifier is also not fully objective.

Augmentation of traditional CIP by our unambiguous translation symmetry detection procedure

Given the inherent subjectivity of the three traditional plane symmetry deviation quantifiers mentioned above, we developed a statistics-rooted measure that quantifies deviations from 2D translation symmetries [7,8]. Such a measure allows for unambiguous identifications of the correct 2D Bravais lattice based on a geometric Akaike information criterion (AIC). As already mentioned above, the problem of subjectivity in utilizing the three traditional plane symmetry deviation quantifiers stems from the fact that the plane symmetry groups are not disjoint (have subgroup/supergroup relationships). Geometric AICs have been successfully used in a wide range of classification schemes involving non-disjoint models [12,13].

In brief, our new assessment method involves the position of the (1,0), (0,1) and (1,1) FC peaks in a 2D transform of an image. These positions are directly related to the reciprocal and direct space lattice parameters of a 2D periodic image, and hence the shapes of the primitive reciprocal and direct space unit cells. The primitive unit (or direct space sub-unit) cells corresponding to 2D Bravais lattices possess the shapes of quadrilaterals, whose vertices x_i are subject to combinations of the constraints listed below:

$$
\begin{array}{lll}
\{1\} & \left.\begin{array}{l}(\mathbf{x}_2-\mathbf{x}_1)\times(\mathbf{x}_4-\mathbf{x}_3)=0\\ (\mathbf{x}_3-\mathbf{x}_1)\times(\mathbf{x}_4-\mathbf{x}_2)=0\end{array}\right\} & \text{Opposite sides are parallel}\\
\{2\} & & \\
\{3\} & \{(\mathbf{x}_3-\mathbf{x}_1)\cdot(\mathbf{x}_4-\mathbf{x}_3)=0\} & \text{Adjacent sides are orthogonal}\\
\{4\} & \{(\mathbf{x}_4-\mathbf{x}_1)\cdot(\mathbf{x}_3-\mathbf{x}_2)=0\} & \text{Diagonals are orthogonal}\\
\{5\} & \{(\mathbf{x}_3-\mathbf{x}_1)\cdot(\mathbf{x}_4-\mathbf{x}_3)=\pm\tfrac{1}{2}|\mathbf{x}_3-\mathbf{x}_1||\mathbf{x}_4-\mathbf{x}_3|\} & \text{Angle is } 60^\circ \text{ or } 120^\circ
\end{array}
\qquad (1)
$$

Specifically, the constraints {1} and {2} together constitute the constraints on the shape of the unit cell of an oblique 2D Bravais lattice. When one combines these with constraint {3}, the set of constraints corresponding to a rectangular (primitive) 2D Bravais lattice is obtained. Similarly, the combination of constrains {1}, {2}, {3} and {4} constitutes the set that constrains the shape of the unit cell of the square 2D Bravais lattice, while the same is true for constraints {1}, {2}, {3} and {5} and the hexagonal 2D Bravais lattice. For the rectangular centered 2D Bravais lattice, its direct space "primitive sub-cell" is constrained by conditions {1}, {2}, and {4}, but not {5} or {3}, i.e. the angle between the primitive lattice vectors is not 60, 90, or 120 degrees.

Note in passing that the constraint set {1} to {4} is given in ref. [11] in order to derive and utilize a geometric AIC for a formally different kind of purpose, i.e. to classify mouse drawn quadrilaterals as either trapezoids, parallelograms, rectangles, rhombuses, or squares. Important for AIC based decisions are only the number of constrains for a set of models that are not disjoint, not how the constraints themselves are actually formulated. In ref. [7], the constraints {1} to {5} are formulated alternatively by the generating 2D point group operators of the five holoedric plane symmetry groups in direct space. The formal equivalence of the geometric AIC procedures for quatrilaterals and the shapes of the unit (or direct space sub-unit) cells of the five 2D Bravais lattices has, thereby, been directly illustrated.

Residuals J are defined as the sums of squared distances from the vertices of the unit cell (in either reciprocal or direct space) of a 2D periodic image to the corresponding vertices of the quadrilaterals that represent the shapes of the unit cells of the 2D Bravais lattices. These vertices are directly related to the

positions of the (1,0), (0,1) and (1,1) FC peaks in the 2D amplitude plot of the Fourier transform of the image. The fourth vertex is set to be identical to the exact position of the (0,0) FC peak.

By definition, J residuals quantify how much the shape of the direct and reciprocal space unit cell of simulated or experimental 2D periodic images differs from the shapes of the quadrilaterals that represent the unit (or direct space sub-unit) cells of the 2D Bravais lattices. On the basis of these residuals, and assuming that deviations from ideal translation symmetry in the experimental image are only due to random errors with a Gaussian distribution of mean zero, the following inequality [7,12] is applicable:

$$\frac{J'}{J} < \frac{2L' - L}{L} \qquad (2),$$

where J' and J are the residuals for two non-disjoint unit (or direct space sub-unit) cell shapes that are subject to a total number of L' and L constraints from the list of relations (1), and $L' > L$. In other words, inequality (2) is the applicable geometric AIC for this scenario.

For instance, a square unit cell is subject to the first four constraints and a primitive rectangular unit cell is only subject to a subset of the square unit cell's constraints, i.e. constraints {1, 2, 3}. In this case, the ratio on the right hand side of inequality (2) is therefore $^5/_3$. That is to say, as long a J' is smaller than $^5/_3$ times J, one is justified to conclude (on a statistically sound basis) that the square unit cell shape with the larger number of constraints correctly models the experimental or simulated image. For concluding a preference of the square unit cell over the rectangular centered (direct space) sub-unit cell, the same $^{J'}/_J < ^5/_3$ ratio applies. Preference of both the primitive rectangular unit cell and the rectangular centered (direct space) sub-unit cell over the oblique unit cell can be concluded on the basis of a $^{J'}/_J$ ratio less than 2. Conclusions such as this can, obviously, only be drawn under the assumptions mentioned above, but then they rest on a statistically sound basis. If there are large uncorrected systematic errors, inequality (2) will not be applicable. Working with a simulated image in this paper that does not contain any kind of orientational, positional or other type of disorder, there are, obviously, no uncorrected systematic errors of this type (while small systematic rest errors remain due to the processing of finite rather than infinite 2D periodic arrays).

In geometric AIC based decisions that identify a square lattice as being preferred, one must have tested for its preference over both the rectangular primitive and the rectangular centered lattice. Additionally, the primitive (direct space) sub-unit cell of the latter of these two lattices needs to be preferred over the hexagonal lattice. Also, one must have checked if choosing both a rectangle and a rhombus over a parallelogram were justified in the first place.

Note that when a perfectly 2D periodic image of infinite extent is Fourier transformed, the (1,0), (0,1) and (1,1) FC peaks will be infinitely sharp Dirac δ-functions, i.e. not spread out at all. When a finite section of such an image is CIP processed, these δ-functions will be convoluted with a "shape function" and the peaks will spread out in a predictable manner. When a finite extent image is not perfectly 2D periodic, the shape of the convoluted FC peaks will be further modified by positional, orientational, and other types of disorder. These effects will all contribute to a "systematic rest error" on the J residuals for an experimental image. Such error bars can be understood as statistical measures on how close the whole CIP procedure, as applied to a finite experimental image, adheres to the crystallographic averaging ideal over a perfectly 2D periodic infinite image.

Applying the standard error propagation formula [14], we calculate error estimates for the errors in our nonlinear residuals $J = J(a,b,\gamma)$ for the non-hexagonal 2D Bravais lattices with respect to specified input data. As a first order estimate:

$$\sigma_J = \sqrt{\left(\frac{\partial J}{\partial a}\cdot\sigma_a\right)^2 + \left(\frac{\partial J}{\partial b}\cdot\sigma_b\right)^2 + \left(\frac{\partial J}{\partial \gamma}\cdot\sigma_\gamma\right)^2} \qquad (3),$$

where σ_a, σ_b and σ_γ are estimates of the random error in each of the independent random variables a, b and γ (our reciprocal or direct lattice parameters), respectively, and σ_J is the estimate of the random error in residual J. (Note that covariance terms are ignored based on the assumption that the random variables are independent and follow a Gaussian distribution of mean zero.) The validity of these results was tested

against established random sampling methods. That comparison supports the estimates gleaned from the application of the standard error propagation formula and will be reported elsewhere. Since we are going to deal only with simulated images below, rough estimates on the error bars of the *J* residuals suffice for this paper.

WORKED EXAMPLE

Figure 1 supports both the description of our new translation symmetry detection procedure and how it enhances the current practices of CIP. The *p4*-symmetry in Fig. 1a is "symmetrically perfect" because we imposed this symmetry on an experimental "nearly-*p4*" STM image [15] using the popular CIP program CRISP [16]. In Fig. 1b we have artificially constructed an image akin to what one would see with three SPM mini-tips shifted laterally with respect to each other, constituting a blunt tip and simultaneously scanning the same sample surface. Although only a hypothetical example, this scenario is not at all uncommon in the experimental praxis, see, e.g. ref. [17]. Obscured images such as Fig. 1b have been discarded in the past, but CIP presents an alternative to recover the crucial average motif information from them.

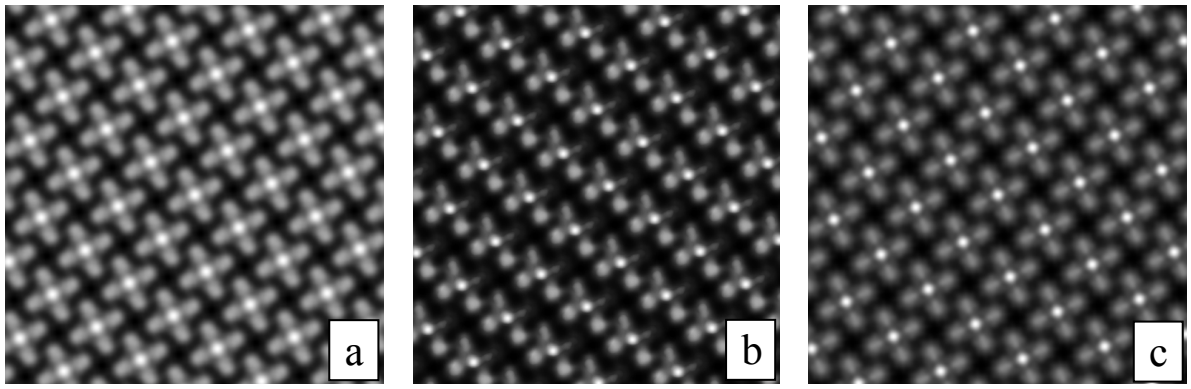

Figure 1. (a) A 512 by 512 pixel image whose *p4*-symmetry is known by design. (The area of this image is approximately 80 nm^2, i.e. slightly smaller than its experimental counterpart in ref. [15]). **(b)** Simulation to model what three mini-tips (a blunt tip) would record when imaging this "sample," constructed in Photoshop. **(c)** CIP reconstruction of (b) with plane symmetry *p4* enforced.

We note that both the unobscured image in Fig. 1a, and the obscured one in Fig. 1b, possess the same translation symmetry, which is that of the square 2D Bravais lattice. This fact is the hallmark of any multiple mini-tip (blunt scanning probe tip) effect on any 2D periodic image and has been demonstrated with mathematical rigor in refs. [8] and [9]. While the obscuration due to multiple tips cannot affect the translation symmetry, it may modify the point symmetry of the 2D periodic motif significantly. Any change of the atomistic details of a scanning probe tip while it is scanning a sample surface cannot change the translation symmetry of the recorded image either. This means that while "individual members" of the 2D periodic motif may possess significant variations in their appearance, they will be arranged in the very same 2D periodic manner throughout the whole of an experimental image. Our geometric AIC procedure can be applied to such images and CIP can be used for the purpose of their crystallographic averaging.

Figure 1c shows the inverse-Fourier image reconstruction of Fig. 1b after *p4* symmetry enforcement in reciprocal space using CRISP. The first three rows of Tables Ia and Ib show the traditional plane symmetry deviation quantifiers from the application of the CRISP program to Fig. 1b. The forth row of these tables give the *J* residuals for the oblique (J_{ob}), rectangular primitive, rectangular centered, and square 2D Bravais lattice as described above and normalized to a lowest possible value of unity for the lowest symmetric unit cell shape, so that the row is labelled J'/J_{ob}. The fact that certain plane symmetries are compatible with certain 2D Bravais lattices is illustrated by the fact that there are fewer entries in the

fourth row of Tables Ia and Ib. (The fact that the J'/J_{ob} values are essentially identical for the non-hexagonal 2D Bravais lattices in Table Ia is an artefact of our image having been simulated under ideal imaging conditions. A more typical result for an experimental image with underling square 2D Bravais lattice would be that the J'/J_{ob} values for the non-hexagonal translation symmetries increase with the number of constraints on the translation symmetry model.)

Plugging the normalized J residuals from Tables Ia and Ib into the applicable geometric AIC inequality (2), we can confirm unambiguously that the simulated data possess the translation symmetry of the square Bravais lattice. (This is of course to be expected because the J residuals are by definition not affected by blunt scanning-probe tip effects and can, therefore, be utilized to detect such effects effectively!)

Our assessment of the three traditional plane symmetry deviation quantifiers is, thus, simplified to a decision between the three plane symmetry groups that are based on a square lattice, i.e. *p4*, *p4mm* and *p4gm*. Evaluating the three traditional plane symmetry deviation quantifiers in the first three rows of Table Ia for plane symmetry groups with square 2D Bravais lattices, it is clear that the underlying plane symmetry is *p4*, which we of course also know to be true from the design history of this image.

(a)	p2	p1m1	p11m	p1g1	p11g	p2mm	p2mg	p2gm	p2gg	c1m1	c11m	c2mm	p4	p4mm	p4gm
A_{res}	n.d.	23.9	23.9	28.3	25.9	23.9	25.9	28.3	31.0	24.9	24.9	24.9	**30.4**	38.8	37.9
φ_{res}	23.3	20.3	21.3	26.0	24.8	35.5	41.8	38.0	32.1	17.5	12.8	22.6	**24.2**	34.8	32.7
A_a/A_e	n.d.	n.d.	n.d.	1.5	0.8	n.d.	0.8	1.5	1.2	1.3	1.3	1.3	**n.d.**	n.d.	1.2
J'/J_{ob}	1.0	1.001 ± 10^{-3}								1.001 ± 10^{-3}			1.001 ± 10^{-3}		

(b)	p3	p3m1	p31m	p6	p6mm
A_{res}	64.9	65.2	65.2	64.9	65.2
φ_{res}	27.3	35.0	33.6	34.4	40.4
A_a/A_e	n.d.	n.d.	n.d.	n.d.	n.d.
J'/J_{ob}	104.5				

Table I. Plane symmetry deviation quantifiers from the application of CRISP to Fig. 1b, along with normalized residuals J used for the unambiguous 2D Bravais lattice identification via our geometric AIC procedure; **(a)** non-hexagonal plane symmetry groups; **(b)** hexagonal plane symmetry groups. The plane symmetry deviation quantifiers for group *p4* are given in bold face.

OUTLOOK

The idea of utilizing geometric AICs in CIP can be developed further to eventually achieve a complete quantification of the deviations of 2D periodic images from the space group symmetries that are allowed in the Euclidian plane. As discussed in ref. [13], key to the application of geometric AICs are residuals in the form of squares of differences and detailed enumerations of numbers of constraints. It seems straightforward to utilize symmetry adapted Fourier series [18] for this purpose. One could define suitable residuals in reciprocal space as the sums of the squares of the differences between symmetry adapted Fourier coefficients and their counterparts as obtained from an ordinary Fourier transform of the 2D periodic image. The numbers of constraints that are applicable would be in a first approximation the multiplicity of the general position [11] in the plane symmetry groups. For better approximations, one would need to include the multiplicities of special positions and weighting factors that account for the relative occupation of these positions in the 2D periodic image to be processed. Alternatively, one may define the residuals in direct space on a per unit cell basis as the sums of the squared differences of the intensity value of the individual pixels of the 2D periodic image in its raw and symmetrized form. The number of constraints would again be given by the multiplicity of the general position.

SUMMARY

A statistically sound procedure for the unambiguous identification of the underlying Bravais lattice of an image of a 2D periodic array of objects (e.g. molecules or atoms and their respective electron density distribution functions) has been presented. While useful in its own right for (*i*) detecting multiple

scanning probe mini-tip effects in experimental images and (*ii*) allowing one to narrow down choices of plane symmetries that an image may possess to those that are compatible with its unambiguously detected 2D Bravais lattice, the underlying ideas around geometric AICs can be further developed to provide a complete solution to the as yet unsolved problem of fully objective decisions on which plane symmetry best models a certain 2D periodic image. Preconditions to make such decisions will be that all systematic errors in the processes of acquiring and processing the image data have been accounted for at a level that systematic rest errors are negligible.

The authors provide the URLs of two recent Master of Science theses, refs. [6] and [7] on CIP for SPM with the belief that they will be useful to the novice in this emerging field. (One can obtain these theses by clicking on the corresponding references in the on line *.pdf version of this paper.)

ACKNOWLEDGMENTS

This research was supported by awards from Portland State University's Venture Development Fund, Portland State University's Internationalization Council, and Faculty Enhancement committee to PM.

REFERENCES

1. P. Moeck, M. Toader, M. Abdel-Hafiez, and M. Hietschold, in *Frontiers of Characterization and Metrology for Nanoelectronics*, edited by D. G. Seiler et al., American Institute of Physics Conference Proceedings Series **1173**, Melville, New York, 2009, pp. 294-298.
2. P. Moeck, J. Straton, M. Toader, and M. Hietschold, *Mater. Res. Soc. Symp. Proc.* **1318**, 149 (2011), doi:10.1557/opl.2011.278.
3. P. Moeck, in *Microscopy: Science Technology, Applications and Education*, Microscopy Book Series No. 4, Vol. **3**, pp. 1951-1962, A. Méndez-Vilas and J. Diaz (editors), Formatex Research Center, 2010, ISBN (13): 978-84-614-6191-2, open access: http://www.formatex.info/microscopy4/1951-1962.pdf.
4. P. Moeck, J. Straton, K. W. Hipps, T. Bilyeu, J.-P. Rabe, U. Mazur, M. Hietschold, M. Toader, *Proc. 11th IEEE International Conference on Nanotechnology*, August 15-18, 2011, Portland, Oregon, USA, pp. 891-896. doi: 10.1109/NANO.2011.6144508.
5. T. Bilyeu, B. Moon Jr., P. Moeck, *Microsc. Microanal.* **18** (Suppl. 2) 934 (2012), doi: http://dx.doi.org/10.1017/S1431927612006526.
6. http://nanocrystallography.research.pdx.edu/media/thesis14acorr.pdf.
7. http://nanocrystallography.research.pdx.edu/media/cms_page_media/6/Taylor_thesis_final.pdf.
8. J. C. Straton, T. T. Bilyeu, B. Moon, and P. Moeck, *Cryst. Res. Technol*., special issue "Advances in Structural and Chemical Imaging", *first publ. on line*: 18 Feb. 2014, DOI: 10.1002/crat.201300240.
9. J. C. Straton, T. T. Bilyeu, B. Moon, and P. Moeck, *IEEE Transactions in Image Processing*, 2014, *in press*.
10. X. Zou and S. Hovmöller, in *Industrial Applications of Electron Microscopy*, Edited by Z. R. Li (Marcel (Dekker Inc., 2003), pp. 583-614.
11. T. Hahn (Ed.), Brief Teaching Edition of Volume A, Space-group symmetry, International Tables for Crystallography, 5th revised ed., International Union of Crystallography (IUCr), Chester 2005.
12. I. Triono, N. Ohta, and K. Kanatani, *IEICE Trans. Inf. & Syst.* **E81-D**, 224 (1998).
13. K. Kanatani, *Int. J. Computer Vision* **26**, 171 (1998).
14. P. R. Bevington and D. K. Robinson, *Data Reduction and Error Analysis for the Physical Sciences*, 3rd ed., McGraw-Hill, 2003, p. 41.
15. U. Mazur, M. Leonetti, W. English, and K. W. Hipps, *J. Phys. Chem. B* **108**, 17003 (2004).
16. S. Hovmöller*, Ultramicroscopy* **41**, 121 (1992).
17. E. V. Iski, A. D. Jewell, H. L. Tierney, G. Kyriakou, and E. C. H. Sykes, *J. Vac. Sci. Technol. A* **29**, 040601 (2011).
18. B. Verberck, *Symmetry* **4**, 379 (2012).